ADVANCED ENERGY MATERIALS
www.advenergymat.de

An Organic Semiconductor Photoelectrochemical Tandem Cell for Solar Water Splitting

*Dan Zhang, Han-Hee Cho, Jun-Ho Yum, Mounir Mensi, and Kevin Sivula**

Photoelectrochemical cells employing organic semiconductors (OS) are promising for solar-to-fuel conversion via water splitting. However, despite encouraging advances with the half reactions, complete overall water splitting remains a challenge. Herein, a robust organic photocathode operating in near-neutral pH electrolyte by careful selections of a semiconducting polymer bulk heterojunction (BHJ) blend and organic charge-selective layer is realized. The optimized photocathode produces a photocurrent density of >4 mA cm^{-2} at 0 V vs the reversible hydrogen electrode (V_{RHE}) for solar water reduction with noticeable operational stability (retaining ≈90% of the initial performance over 6 h) at pH 9. Combining the optimized BHJ photocathode with a benchmark BHJ photoanode leads to the demonstration of a large-area (2.4 cm^2) organic photoelectrochemical tandem cell for complete solar water splitting, with a predicted solar-to-hydrogen (STH) conversion efficiency of 0.8%. Under unassisted two-electrode operation (1 Sun illumination) a stabilized photocurrent of 0.6 mA and an STH of 0.3% are observed together with near unity Faradaic efficiency of H_2 and O_2 production.

1. Introduction

The global-scale artificial photosynthesis of solar-fuels is urgently needed to progress toward a low-carbon energy economy.[1] Solar-driven green hydrogen (H_2) production via water splitting stands out as a promising approach, and using photoelectrochemical (PEC) or heterogenous photocatalytic (PC) systems can potentially realize green H_2 in an economically competitive and scalable manner. Indeed, since the light-harvesting semiconductor material is placed in direct contact with water in the PEC and PC approaches the system complexity is minimized.[2–4] Because an ideal single semiconductor whose energy band positions straddle the water reduction and oxidation potentials while maximizing solar energy collection remains elusive, the dual-absorber approaches (i.e., the PEC tandem cell[5–7] and PC Z-scheme[8–10]) are currently under intense development. In a PEC tandem cell, a photocathode and a photoanode are configured in series, and both absorb part of the incident sunlight to drive the water reduction and oxidation reactions, respectively, while exchanging charges via a direct electrical connection. Analogously in a PC Z-Scheme, hydrogen evolution particles and oxygen evolution particles drive the water splitting reactions while electronically communicating via a redox shuttle.

Despite decades of research in these systems, the demonstration of high-performance solar water splitting with inexpensive and scalable systems remains challenging in part due to the absence of ideal semiconductor materials.[11] Organic semiconductors (OSs) are rapidly emerging as promising candidates to tackle this challenge.[12–17] OSs are characterized by polymers or small molecules with extended pi-conjugation of carbon bonds and possess many promising properties including energy levels that can be easily tailored through molecular engineering, and excellent light harvesting properties derived from relatively high molar extinction coefficients.[18] In addition, OSs can be solution-processed at ambient temperatures, which facilitates the economical fabrication of large-area thin film devices[19] or the scalable production of nanoparticle photocatalysts.[20] Furthermore, as well established in the field of organic photovoltaics, when an electron donating OS is placed in contact with an electron accepting OS to form a bulk heterojunction (BHJ) structure (where they are well-intermixed at a ≈10 nm length scale), free charge carriers are efficiently photogenerated and separated—a process that can be easily adjusted by varying the combination of donor and acceptor.[21] Indeed, this BHJ concept has recently been leveraged with photoelectrodes and photocatalysts to achieve breakthrough performance in either solar-driven water reduction[22–24] or water oxidation.[25,26] Moreover, the stability of the OS-based PEC devices has been addressed.[24] Despite this progress, overall water splitting has not been demonstrated with OS-based PEC or PC systems that leverage the BHJ concept.

D. Zhang, H.-H. Cho, J.-H. Yum, K. Sivula
Laboratory for Molecular Engineering of Optoelectronic Nanomaterials
Institute of Chemical Sciences and Engineering
École Polytechnique Fédérale de Lausanne (EPFL)
Station 6, Lausanne 1015, Switzerland
E-mail: kevin.sivula@epfl.ch

H.-H. Cho
School of Materials Science and Engineering
Ulsan National Institute of Science and Technology (UNIST)
Ulsan 44919, Republic of Korea

M. Mensi
Institute of Chemical Sciences and Engineering
École Polytechnique Fédérale de Lausanne (EPFL)
Valais Wallis CH-1951 Sion, Switzerland

The ORCID identification number(s) for the author(s) of this article can be found under https://doi.org/10.1002/aenm.202202363.

DOI: 10.1002/aenm.202202363

Indeed, major preconditions must be satisfied to assemble an overall water splitting tandem or Z-scheme device. For the PEC tandem cell, in particular, the photocathode and photoanode should be stable in the same electrolyte at the same pH (ideally near-neutral) while also providing sufficient driving force for water reduction and oxidation reaction, respectively. Moreover, the photocurrent onset potentials of the photocathode and photoanode should be sufficiently positive and negative, respectively, so that both photoelectrodes produce decent photocurrent at the operating potential (where the current-voltage curves of photoelectrodes are overlapped), allowing applied-bias free operation of the device.[5] Whereas the present state-of-the-art organic photoanode driving the oxygen evolution reaction (OER) displayed a low onset potential of + 0.2 V vs the reversible hydrogen electrode (V_{RHE}) in aqueous electrolyte buffered at near-neutral pH (pH 9),[25] recent high-performance OS-based photocathodes have either shown unsuitable onset potentials (typically, +0.5 –0.67 V_{RHE}) or been employed in strongly acidic conditions (pH ≈1).[24,27–29] Since the energy levels of OS-based materials in aqueous electrolyte typically do not shift with pH,[30,31] the driving force for water reduction will unfavorably decrease for OS-based photocathodes at higher pH. Therefore, a main limitation toward the demonstration of overall water splitting with an OS-based tandem cell is the realization of an OS photocathode that exhibits sufficient onset potential with operational stability in near-neutral pH electrolyte. Herein, we report advances in the device engineering of an OS BHJ photocathode that allow for the first demonstration of bias-free solar-driven water splitting by an OS-based PEC tandem cell.

2. Results and Discussion

To first address the issue of photocathode onset potential in near-neutral pH electrolyte, we judiciously selected semiconducting polymers to provide both efficient free-charge generation and a more positive onset potential for water reduction (see **Figure 1**a for chemical structures). A non-fullerene naphthalenediimide(NDI)-based acceptor, coded as PNDIHDT (Acceptor 1), was selected due to its lowest unoccupied molecular orbital (LUMO) level, which is expected to be suitable for water reduction over a wide range of pH (See Figure 1b for the estimated energy levels compared to the water reduction

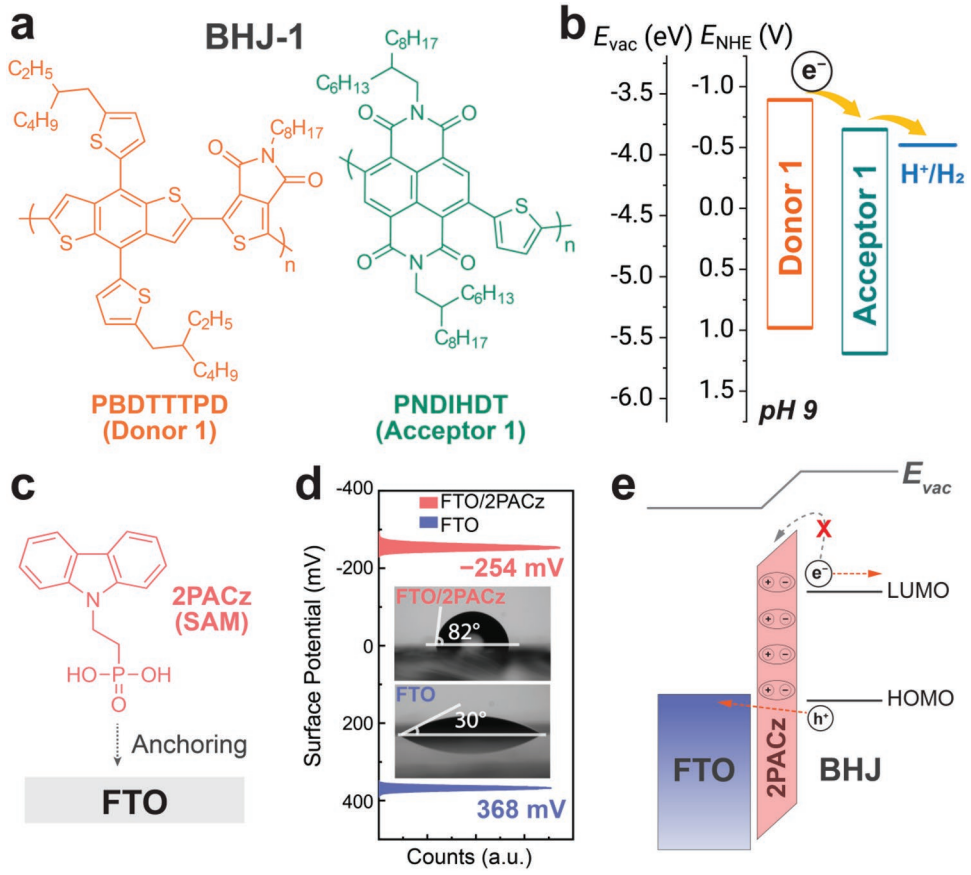

Figure 1. a) Chemical structures of PBDTTTPD (Donor 1):PNDIHDT (Acceptor 1). b) Estimated energy levels of Donor 1 and Acceptor 1 compared to the water reduction potential at pH 9 vs the vacuum energy level (E_{vac}) and normal hydrogen electrode (E_{NHE}). c) Chemical structure and schematic of 2PACz anchoring to FTO. d) Histogram plot of the surface potential of FTO and FTO/SAM substrates as measured by Kelvin probe force microscopy, the inset images show the water contact angle. e) Energy levels of FTO, 2PACz-SAM, and BHJ are shown relative to E_{vac} considering the effect of interfacial dipole (with positive charge end pointing toward FTO and negative charge end pointing to BHJ), which is expected to promote efficient hole extraction but block back-transfer of electrons.

potential at pH 9). Furthermore, a benzodithiophene-based donor polymer coded as PBDTTTPD (Donor 1) was chosen for its deeper highest occupied molecular orbital (HOMO) level as the photovoltage is generally proportional to energy difference between the LUMO level of an acceptor and the HOMO level of a donor. Compared to a previous polymer BHJ employed as an OS photocathode at pH 1 using the polymers coded as PTB7-Th and PDI-V (see structures in Figure S1a, Supporting Information), we anticipated a larger photovoltage for a photocathode prepared from BHJ-1 (Donor 1:Acceptor 1) (See Figure S1b, Supporting Information for a comparison of the energy levels). Moreover, energy alignment of BHJ-1 with respect to water reduction reaction at pH 9 ensures sufficient driving force for electron transfer at the photocathode surface (Figure 1b). Thus, a photocathode based on the BHJ-1 is expected to operate efficiently at near-neutral pH while showing more positive photocurrent onset potential for water reduction.

Before examining the H_2 evolution performance, it was necessary to address the photocathode architecture to ensure its compatibility with near-neutral aqueous conditions. Indeed, the previously-used[24] charge-selective layer (CSL) material, MoO_3, is not compatible with pH > 2. Alternatively, we employed the organic molecule (2-(9*H*-carbazol-9-yl)ethyl)phosphonic acid[32] (2PACz, molecular structure in Figure 1c), which consists of the hole-transporting carbazole moiety[33] linked to a phosphonic acid functionality, and is capable of forming a self-assembled monolayer (SAM) on the transparent conducting F-doped SnO_2 (FTO) substrate.[34,35] To verify the successful deposition of 2PACz, the surface properties of 2PACz-modified FTO were first examined using atomic force microscopy (AFM) and Kelvin probe force microscopy (KPFM). The monolayer assembly of 2PACz (2PACz-SAM) on FTO did not induce any change in morphology by AFM (see Figure S2, Supporting Information) as supported by the similar root-mean-square roughness of 13.8 nm for FTO and 13.7 nm for the 2PACz-modified FTO. Interestingly, the surface potential as measured by KPFM differed significantly between the FTO and the 2PACz-modified FTO (Figure 1d). While both substrates showed narrow distributions of contact potential difference (V_{CPD}) over the imaged surface, the average V_{CPD} for FTO and FTO/2PACz-SAM was +368 and −254 mV, respectively, demonstrating the effectiveness of electronic modification using the 2PACz-SAM. It is expected that the oriented 2PACz on FTO gives rise to an interfacial dipole at the surface that results in an electric field and a subsequent shift of substrate work function, as illustrated in Figure 1e. Indeed, ultra-violet photoelectron spectroscopy (UPS, see Figure S3, Supporting Information) confirms the change in surface energetics after the modification by 2PACz. The shift of the work function induced by the dipole moment of the 2PACz-SAM was measured to be ≈340 meV, which implies better energy level alignment to the HOMO level of the BHJ layer. In addition to surface energetics, the 2PACz-treated FTO also presented a significantly more hydrophobic surface, as shown by contact angle measurements with water (Figure 1d, inset images). The FTO/SAM substrate showed an increased water contact angle of 82° compared to bare FTO with a contact angle of 30°. Such a change in surface wetting properties is important since a hydrophobic surface is expected to facilitate the coating and adhesion of the hydrophobic polymer BHJ to the substrate.

To establish the effectiveness of the 2PACz-SAM on the photocathode performance and demonstrate the importance of the BHJ energy levels for operation at near-neutral pH, linear scanning voltammetry (LSV) for solar water reduction was performed in aqueous 0.1 M sodium borate (NaBi) buffer (pH 9) under simulated 1-Sun illumination. The photocathode configuration used is shown schematically in **Figure 2**a and consisted of a glass-FTO substrate (with or without the 2PACz SAM modification), the spin-coated BHJ as the photoactive layer, and spray-coated RuO_2 as a H_2 evolution reaction (HER) catalyst. As shown by LSV curves in Figure 2b taken under intermittent illumination, an FTO/SAM/BHJ-1/RuO_2 photocathode produced a photocurrent density (J_{ph}) of 4.6 mA cm^{-2} at 0 V_{RHE}. In contrast, a photocathode fabricated without the SAM (FTO/BHJ-1/RuO_2) showed negligible photocurrent, indicating the importance of the CSL on the charge extraction at the FTO/BHJ interface. More importantly, a photocathode prepared with MoO_3 CSL exhibited a lower photocurrent (Figure S4, Supporting Information) and poor mechanical stability as evidenced by the detachment of the BHJ photoactive layer from the electrode after a single LSV scan while the BHJ film deposited on the 2PACz-SAM remained intact (Figure S5, Supporting Information). Furthermore, to confirm the importance of the polymer energy levels in the BHJ system, we next compared photocathodes based on BHJ-1 to the previously-reported BHJ of PTB7-Th:PDI-V (BHJ-2). Interestingly, under constant illumination at pH 9, the FTO/SAM/BHJ-1/RuO_2 photocathode exhibited a photocurrent onset potential of nearly +1.0 V_{RHE} (Figure 2c) whereas the photocurrent of the FTO/SAM/BHJ-2/RuO_2 photocathode did not onset until ≈+0.6 V_{RHE} and the J_{ph} was only 3.2 mA cm^{-2} at 0 V_{RHE}. The observations in Figure 2b,c thus demonstrate the importance of the CSL engineering and the BHJ energy levels tunning on obtaining a photocathode better suited for operation in a PEC tandem cell.

Further evaluation of our optimized photocathode (the FTO/SAM/BHJ-1/RuO_2 photocathode, simply denoted as the BHJ-1 photocathode hereafter) with respect to reproducibility showed similar performance of five separate photocathodes fabricated under similar conditions (Figure S6a, Supporting Information). Moreover, the operational stability was evaluated by chronoamperometry (CA) measurements at 0 V_{RHE}. As shown in Figure 2d, the J_{ph} of the BHJ-1 photocathode is found to retain ≈90% of its initial value after continuous operation for 6 h. We note the "sawtooth" pattern of the CA data was due to the recovery of catalyst surface after hydrogen gas bubble detachment. The stability reported in Figure 2d was also found to be very reproducible as displayed in Figure S6b, (Supporting Information) with five different replicate devices.

Electrolyte compatibility was further examined with the BHJ-1 photocathode over a range of pH. At pH 6 in a 0.1 M potassium phosphate (KPi) buffer electrolyte the performance was similar to pH 9, however, strongly acidic or basic conditions were detrimental for the photocathode stability (Figure S7, Supporting Information). The poorer longevity of the photocurrent in these cases is reasonably due to the detachment of the 2PACz-SAM, as chemically bonded phosphonic acid groups undergo a desorption process under these conditions.[36–38] While SAM molecules with stronger binding groups[38–40] could survive under harsh pH conditions (giving a direction

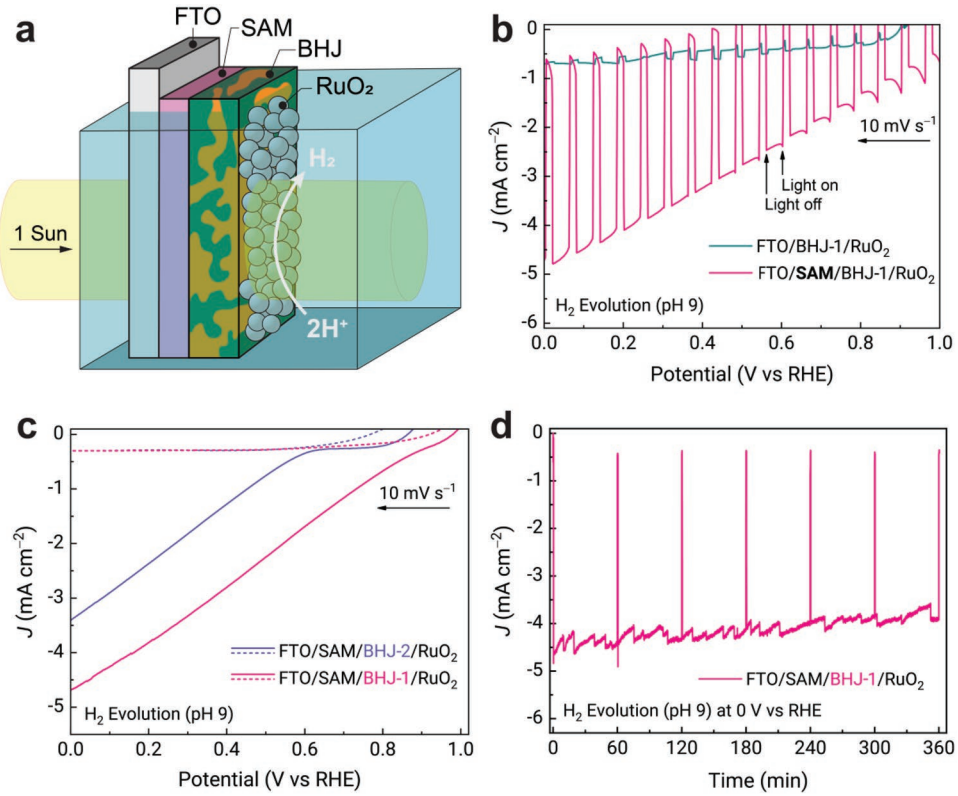

Figure 2. a) Scheme of the FTO/SAM/BHJ/RuO_2 photocathode for solar water reduction. b) LSV scans (under intermittent illumination) of the photocathodes without (green) and with (pink) 2PACz-SAM CSL for water reduction in 0.1 M NaBi buffer electrolyte (pH 9). c) LSV scans of the photocathodes with BHJ-1 (pink) and BHJ-2 (violet) as active layer for water reduction under continuous illumination (solid) and dark (dash) in 0.1 M NaBi buffer electrolyte (pH 9). d) CA curves (at 0 V_{RHE}) of FTO/SAM/BHJ-1/RuO_2 photocathode in 0.1 M NaBi buffer electrolyte (pH 9).

for future development), the demonstrated performance of the BHJ-1 photocathode at near-neutral pH is sufficient to proceed with the demonstration of an organic PEC tandem cell.

To realize an all-BHJ-based PEC tandem cell, we fabricated both photocathode and photoanode with relatively large active areas of 1.2 × 2 cm^2. For the photoanode, we chose the donor:acceptor blend with the polymers coded as PBDTTTPD:PNDITCVT (see structures in Figure S8, Supporting Information), which we will call BHJ-3 in this work, and used a similar photoanode architecture to the previous report (FTO/mesoporous ZnO(mZnO)/BHJ-3/PTAA/Li-modified IrO_2). We chose to place the photoanode behind the photocathode since the stability of the photoanode is increased at lower light intensity.[25] Thus, the polymer BHJ photocathode and photoanode receive the simulated 1-Sun illumination in succession from substrate side (FTO side) as shown in the schematic in **Figure 3**a. Photographs of the tandem configuration are shown in Figure 3b. We note that the photocathode optimization described in the paragraphs above was performed in anticipation of the employed device configuration and the active layer was kept thin so as to ensure sufficient light transmission to the photoanode. Indeed, over the visible wavelength range (400–700 nm), the complete photocathode exhibited a transmittance ranging from 25% to 50% (see Figure S9, Supporting Information). Accordingly, since the polymers of BHJ-3 absorb similar wavelengths of light compared to BHJ-1, the photocurrent delivered by the photoanode was lower than the previous report. An LSV of the photoanode in place behind the photocathode is shown in comparison to the LSV of the photocathode in Figure 3c. Note that the absolute value of the photocurrent is used for the photoelectrodes so that the predicted tandem cell operating point can be easily discerned as the intersection between the LSV curves (operating photocurrent, I_{op} of 1.54 mA and operating potential, E_{op} at +0.64 V_{RHE}). Under bias-free two-electrode operational measurements, the tandem cell generated a stabilized photocurrent of ≈0.6 mA after an initial photocurrent transient and remained over 0.4 mA after 2 h of continuous operation (Figure 3d). We note that the illumination was briefly turned off to demonstrate the low dark current of the device. Furthermore, H_2 and O_2 bubbles on organic photoelectrodes were clearly observed during operation (Figure 3b).

To confirm the H_2 and O_2 production and estimate Faradaic efficiency, gas chromatography (GC) measurements were conducted. To accommodate our sealed GC measurement cell, a smaller active area (0.25 cm^2) and a face-to-face configuration for the photoelectrodes was adopted. Despite these differences, the performance was similar (see the corresponding current density curve during GC measurements in Figure S10, Supporting Information) and the measured amount of H_2 and O_2 gave Faradaic efficiencies of 102 ± 5% for H_2 and 91 ± 9% O_2 evolution (Figure 3e) as an average over seven measurements

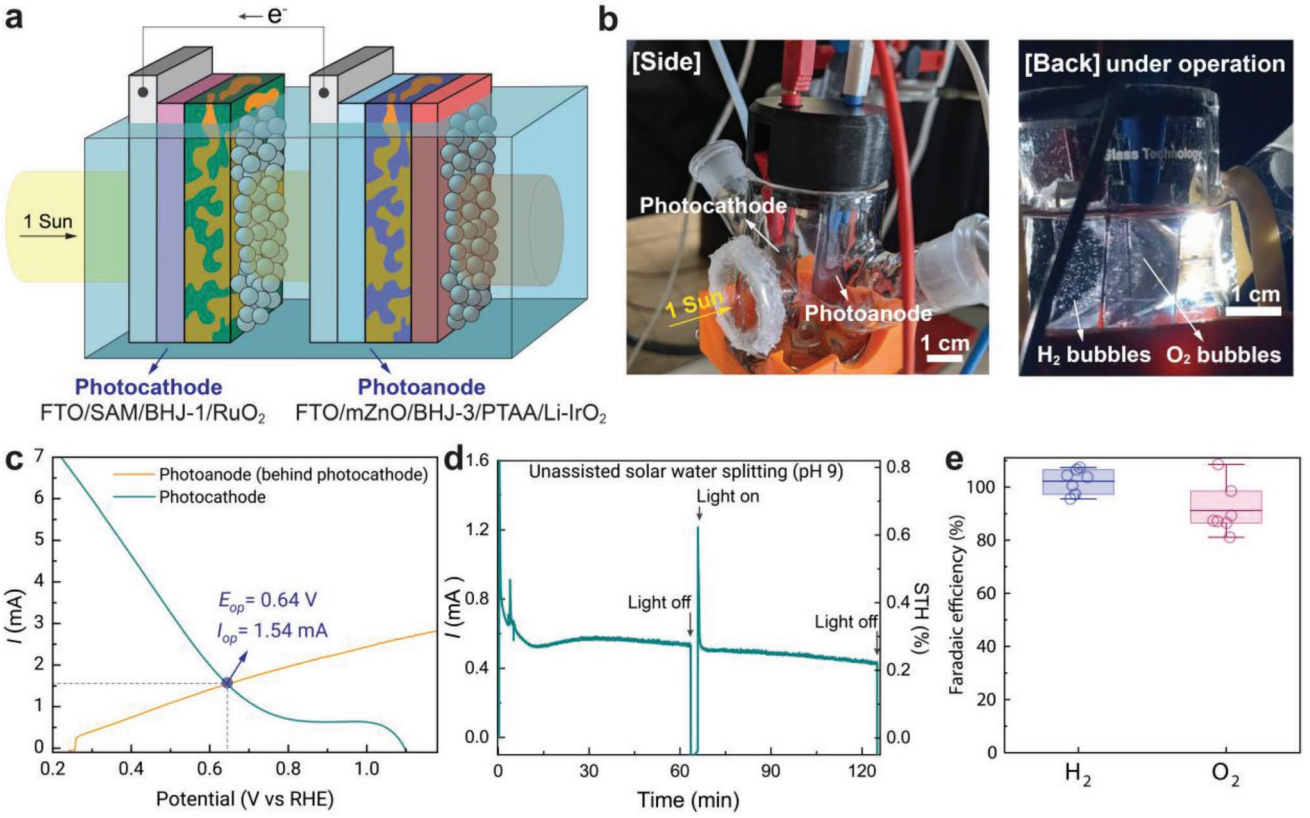

Figure 3. a) Scheme of tandem cell with FTO/SAM/BHJ-1/RuO_2 photocathode for water reduction and FTO/mZnO/BHJ-3/PTAA/Li-IrO_2 photoanode for water oxidation. b) Digital images of the large-area tandem cell configuration (left) and bubble formation during operation (right). c) LSV scans (under continuous illumination) of the photocathode and photoanode (behind photocathode) in 0.1 M NaBi buffer electrolyte (pH 9). Active area = 2.4 cm^2. d) Photocurrent (at zero bias) and STH efficiency of the tandem cell in 0.1 M NaBi buffer electrolyte (pH 9). e) Faradaic efficiency of the HER on the photocathode (violet) and OER on the photoanode (pink) detected by GC, with standard amount of H_2 and O_2 calibrated using platinum foil.

(see the cumulative amounts of H_2 and O_2 in Figure S11, Supporting Information), suggesting near unity turnover of the complete light-driven water splitting reaction. Moreover, solar-to-hydrogen efficiency (η_{STH}) was calculated according to Equation S1 (Supporting Information). An initial η_{STH} was estimated to be 0.8% based on the operating photocurrent of 1.54 mA as shown in Figure 3c, and the stabilized photocurrent of ≈0.6 mA (Figure 3d) after an initial photocurrent transient delivered the actual η_{STH} of ≈0.3%. While this performance is modest, it should be noted that other demonstrations of true PEC tandem cells (where the light absorbers are in direct contact with the water) with competing materials (e.g., metal oxides) give similar values ≈1%.[7] Moreover, we emphasize that our work represents the first successful demonstration of an organic semiconductor BHJ photoelectrochemical tandem cell for complete solar-driven water splitting with an appreciable η_{STH}. Follow-up efforts are needed to further optimize the BHJ components and interfacial layers to increase the complementarity of solar light harvesting (i.e., to raise the photocurrent of the second photoelectrode). The molecular tunability of polymer semiconductors offers opportunity in this aspect to advance this system toward the final goal of efficient, robust, and low-cost production of hydrogen on a global large-scale.

3. Conclusion

In summary, we established a simple bulk heterojunction photocathode that can efficiently reduce water to hydrogen in a pH 9 electrolyte by judicious organic semiconductor selection and replacing the conventional metal oxide hole transporting layer with an organic self-assembled monolayer charge selective layer. The SAM of 2PACz offers increased pH compatibility compared to metal oxide-based hole transporting layers (that are prone to chemical corrosion in aqueous electrolyte) and other advantages such as minimal parasitic light absorption, low material consumption, and simpler preparation at lower temperatures, making SAM CSLs attractive for the fabrication of scalable organic photocathodes. The obtained photocathode delivered a photocurrent density of 4.6 mA cm^{-2} and stable operation for at least 6 h while retaining ≈90% of the initial photocurrent. Together with a previously-established photoanode, for the first time, an all-polymer photoelectrochemical tandem cell was successfully assembled for unbiased solar water splitting. The tandem cell exhibited an operational photocurrent density of ca. 0.3–0.4 mA cm^{-2}, with the products confirmed by gas chromatography at nearly 100% Faradaic efficiency. Our work sets a new benchmark for the potential production of low-cost solar fuel.

Supporting Information

Supporting Information is available from the Wiley Online Library or from the author.

Acknowledgements

D.Z. and H.-H.C. contributed equally to this work. The authors acknowledge the Swiss National Science Foundation (project number 200020_185041) for support. H.-H. Cho thanks the National Research Foundation of Korea (NRF) for a grant funded by the Korea government (Ministry of Science and ICT, MSIT) (No. 2022R1F1A107329711)

Open access funding provided by Ecole Polytechnique Federale de Lausanne.

Conflict of Interest

The authors declare no conflict of interest.

Data Availability Statement

The data that support the findings of this study are available from the corresponding author upon reasonable request.

Keywords

organic semiconductors, photoanodes, photocathodes, solar water splitting

Received: July 12, 2022
Revised: August 17, 2022
Published online:

[1] S. J. Davis, N. S. Lewis, M. Shaner, S. Aggarwal, D. Arent, I. L. Azevedo, S. M. Benson, T. Bradley, J. Brouwer, Y.-M. Chiang, C. T. M. Clack, A. Cohen, S. Doig, J. Edmonds, P. Fennell, C. B. Field, B. Hannegan, B.-M. Hodge, M. I. Hoffert, E. Ingersoll, P. Jaramillo, K. S. Lackner, K. J. Mach, M. Mastrandrea, J. Ogden, P. F. Peterson, D. L. Sanchez, D. Sperling, J. Stagner, J. E. Trancik, et al, *Science* **2018**, *360*, eaas9793.
[2] Y. Tachibana, L. Vayssieres, J. R. Durrant, *Nat. Photonics* **2012**, *6*, 511.
[3] T. Hisatomi, K. Domen, *Nat. Catal.* **2019**, *2*, 387.
[4] B. A. Pinaud, J. D. Benck, L. C. Seitz, A. J. Forman, Z. Chen, T. G. Deutsch, B. D. James, K. N. Baum, G. N. Baum, S. Ardo, H. Wang, E. Miller, T. F. Jaramillo, *Energy Environ. Sci.* **2013**, *6*, 1983.
[5] M. S. Prévot, K. Sivula, *J. Phys. Chem. C* **2013**, *117*, 17879.
[6] K. Zhang, M. Ma, P. Li, D. H. Wang, J. H. Park, *Adv. Energy Mater.* **2016**, *6*, 1600602.
[7] Y. Chen, X. Feng, Y. Liu, X. Guan, C. Burda, L. Guo, *ACS Energy Lett.* **2020**, *5*, 844.
[8] P. Zhou, J. Yu, M. Jaroniec, *Adv. Mater.* **2014**, *26*, 4920.
[9] Z. Wang, C. Li, K. Domen, *Chem. Soc. Rev.* **2019**, *48*, 2109.
[10] J. Abdul Nasir, A. Munir, N. Ahmad, T. ul Haq, Z. Khan, Z. Rehman, *Adv. Mater.* **2021**, *33*, 2105195.
[11] K. Sivula, R. van de Krol, *Nat. Rev. Mater.* **2016**, *1*, 15010.
[12] L. Yao, A. Rahmanudin, N. Guijarro, K. Sivula, *Adv. Energy Mater.* **2018**, *8*, 1802585.
[13] L. Steier, S. Holliday, *J. Mater. Chem. A* **2018**, *6*, 21809.
[14] Y. Wang, A. Vogel, M. Sachs, R. S. Sprick, L. Wilbraham, S. J. A. Moniz, R. Godin, M. A. Zwijnenburg, J. R. Durrant, A. I. Cooper, J. Tang, *Nat. Energy* **2019**, *4*, 746.
[15] H.-H. Cho, K. Sivula, *Trends Chem* **2022**, *4*, 93.
[16] C. Zhao, Z. Chen, R. Shi, X. Yang, T. Zhang, *Adv. Mater.* **2020**, *32*, 1907296.
[17] Y. Fang, Y. Hou, X. Fu, X. Wang, *Chem. Rev.* **2022**, *122*, 4204.
[18] H. Bronstein, C. B. Nielsen, B. C. Schroeder, I. McCulloch, *Nat. Rev. Chem.* **2020**, *4*, 66.
[19] F. C. Krebs, T. Tromholt, M. Jørgensen, *Nanoscale* **2010**, *2*, 873.
[20] N. P. Holmes, S. Chambon, A. Holmes, X. Xu, K. Hirakawa, E. Deniau, C. Lartigau-Dagron, A. Bousquet, *Curr. Opin. Colloid Interface Sci.* **2021**, *56*, 101511.
[21] A. Facchetti, *Mater. Today* **2013**, *16*, 123.
[22] J. Kosco, M. Bidwell, H. Cha, T. Martin, C. T. Howells, M. Sachs, D. H. Anjum, S. G. Lopez, L. Zou, A. Wadsworth, W. Zhang, L. Zhang, J. Tellam, R. Sougrat, F. Laquai, D. M. DeLongchamp, J. R. Durrant, I. McCulloch, *Nat. Mater.* **2020**, *19*, 559.
[23] J. Kosco, S. Gonzalez-Carrero, C. T. Howells, T. Fei, Y. Dong, R. Sougrat, G. T. Harrison, Y. Firdaus, R. Sheelamanthula, B. Purushothaman, F. Moruzzi, W. Xu, L. Zhao, A. Basu, S. De Wolf, T. D. Anthopoulos, J. R. Durrant, I. McCulloch, *Nat. Energy* **2022**, *7*, 340.
[24] L. Yao, N. Guijarro, F. Boudoire, Y. Liu, A. Rahmanudin, R. A. Wells, A. Sekar, H.-H. Cho, J.-H. Yum, F. L.e Formal, K. Sivula, *J. Am. Chem. Soc.* **2020**, *142*, 7795.
[25] H.-H. Cho, L. Yao, J.-H. Yum, Y. Liu, F. Boudoire, R. A. Wells, N. Guijarro, A. Sekar, K. Sivula, *Nat. Catal.* **2021**, *4*, 431.
[26] T. H. Lee, R. R. Rao, R. A. Pacalaj, A. A. Wilson, J. R. Durrant, *Adv. Energy Mater.* **2022**, *12*, 2103698.
[27] L. Francàs, E. Burns, L. Steier, H. Cha, L. Solà-Hernández, X. Li, P. S. Tuladhar, R. Bofill, J. García-Antón, X. Sala, J. R. Durrant, *Chem. Commun.* **2018**, *54*, 5732.
[28] L. Steier, S. Bellani, H. C. Rojas, L. Pan, M. Laitinen, T. Sajavaara, F. D. Fonzo, M. Grätzel, M. R. Antognazza, M. T. Mayer, *Sustain. Energy Fuels* **2017**, *1*, 1915.
[29] A. Alfano, A. Mezzetti, F. Fumagalli, C. Tao, E. Rovera, A. Petrozza, F. Di Fonzo, *iScience* **2021**, *24*, 102463.
[30] L. Yao, Y. Liu, H.-H. Cho, M. Xia, A. Sekar, B. P. Darwich, R. A. Wells, J.-H. Yum, D. Ren, M. Grätzel, N. Guijarro, K. Sivula, *Energy Environ. Sci.* **2021**, *14*, 3141.
[31] P. Bornoz, M. S. Prévot, X. Yu, N. Guijarro, K. Sivula, *J. Am. Chem. Soc.* **2015**, *137*, 15338.
[32] A. Al-Ashouri, A. Magomedov, M. Roß, M. Jošt, M. Talaikis, G. Chistiakova, T. Bertram, J. A. Márquez, E. Köhnen, E. Kasparavičius, S. Levcenco, L. Gil-Escrig, C. J. Hages, R. Schlatmann, B. Rech, T. Malinauskas, T. Unold, C. A. Kaufmann, L. Korte, G. Niaura, V. Getautis, S. Albrecht, *Energy Environ. Sci.* **2019**, *12*, 3356.
[33] M. S. Kang, S. D. Sung, I. T. Choi, H. Kim, M. Hong, J. Kim, W. I. Lee, H. K. Kim, *ACS Appl. Mater. Interfaces* **2015**, *7*, 22213.
[34] P. J. Hotchkiss, S. C. Jones, S. A. Paniagua, A. Sharma, B. Kippelen, N. R. Armstrong, S. R. Marder, *Acc. Chem. Res.* **2012**, *45*, 337.
[35] S. A. Paniagua, A. J. Giordano, O. L. Smith, S. Barlow, H. Li, N. R. Armstrong, J. E. Pemberton, J.-L. Brédas, D. Ginger, S. R. Marder, *Chem. Rev.* **2016**, *116*, 7117.
[36] K. L. Materna, R. H. Crabtree, G. W. Brudvig, *Chem. Soc. Rev.* **2017**, *46*, 6099.
[37] E. Bae, W. Choi, J. Park, H. S. Shin, S. B. Kim, J. S. Lee, *J. Phys. Chem. B* **2004**, *108*, 14093.
[38] L. A. Martini, G. F. Moore, R. L. Milot, L. Z. Cai, S. W. Sheehan, C. A. Schmuttenmaer, G. W. Brudvig, R. H. Crabtree, *J. Phys. Chem. C* **2013**, *117*, 14526.
[39] W. R. McNamara, R. C. S. Iii, G. Li, C. Richter, L. J. Allen, R. L. Milot, C. A. Schmuttenmaer, R. H. Crabtree, G. W. Brudvig, V. S. Batista, *Energy Environ. Sci.* **2009**, *2*, 1173.
[40] W. R. McNamara, R. L. Milot, H. Song, R. C. S. Iii, V. S. Batista, C. A. Schmuttenmaer, G. W. Brudvig, R. H. Crabtree, *Energy Environ. Sci.* **2010**, *3*, 917.